Coral Reefs (2006) 25: 369–381
DOI 10.1007/s00338-006-0121-x

REPORT

C. D. Storlazzi · E. K. Brown · M. E. Field

The application of acoustic Doppler current profilers to measure the timing and patterns of coral larval dispersal

Received: 8 August 2005 / Accepted: 12 April 2006 /

Abstract An experiment was conducted along the reefs off west Maui, Hawaii, during the summer of 2003 to monitor the spawning of the reef-building coral *Montipora capitata* and to determine the role of ocean currents in dispersing the larvae from the natal reef. Instruments documented the environmental forcing during the coral spawning season; drifters were deployed on three successive nights following direct observations of coral spawning. Both the timing and relative magnitude of the coral spawning were identifiable in acoustic backscatter data and correlated to plankton tow data. Each drifter track showed that the surface water containing coral eggs and planula larvae were transported rapidly offshore and not locally retained. Wind and current patterns during the previous year and during subsequent coral spawning events later in the summer were similar to those observed during the drifter releases. This suggests that the trajectories observed during the focused experiment are representative of the general pattern of larval dispersal off west Maui. These findings demonstrate the application of acoustic profilers for remotely imaging coral spawning and predicting their initial dispersal patterns.

Keywords Coral spawning · Coral larvae · Currents · Drifters · Acoustic backscatter · *Montipora capitata*

Communicated by Ecology Editor P.J. Mumby

C. D. Storlazzi (✉) · M. E. Field
US Geological Survey, Pacific Science Center,
400 Natural Bridges Drive, Santa Cruz, CA 95060, USA
E-mail: cstorlazzi@usgs.gov
Tel.: +1-831-4274747
E-mail: mfield@usgs.gov

E. K. Brown
National Park Service, Kalaupapa National Historic Park,
P.O. Box 2222, Kalaupapa, HI 96742, USA
E-mail: eric_brown@nps.gov
Tel.: +1-808-5766802

Introduction

Larval dispersal commonly controls the spatial distribution of marine organisms that have planktonic larval stages and are sessile or highly sedentary as adults. A better understanding of the timing and patterns of larval dispersal enhances our understanding of population connectivity (Swearer et al. 2002) and new habitat colonization or recolonization of habitat after disturbance (Grigg and Maragos 1974), whether natural or anthropogenic (Loya 1976). Currents that carry larvae may also convey material that is detrimental to marine organisms, including contaminants, excess nutrients and fine-grained particulates (Fabricius 2005). Understanding circulation patterns in the vicinity of coral reefs, therefore, has multiple important applications. Despite the importance of dispersal patterns in marine systems to resource managers and scientists, they remain not well documented.

A number of previous studies have investigated coral spawning and larval dispersal, using tools ranging from oceanographic instruments and numerical models (Sammarco and Andrews 1988; Wolanski et al. 1989; Oliver et al. 1992) to the use of satellite- or radio-tracked drifters (Lugo-Fernandez et al. 2001; Nadaoka et al. 2002). Most of the previous experiments, however, have either lacked long-term, in situ oceanographic observations to determine the degree to which short-term model runs and/or drifter trajectories are representative of the dominant patterns. This paper shows that acoustic Doppler current profilers (ADCPs), which are becoming the standard for current measurements in the coastal zone, cannot only make long-term measurements of current speeds and directions, but also have the potential to record the timing, magnitude and initial dispersal pathways of coral larvae from a reef.

Fringing reef tracts with high coral coverage are found off west Maui, Hawaii, USA, in relatively close proximity (~2 km) to suitable coral habitat (hard, consolidated substrate) with low coral coverage. One question of interest to both scientists and resource managers is whether the lack of high live coral coverage along many sections of west Maui was simply due to a lack of coral larvae being transported to those areas. To address this question, an experiment was conducted in the summer of 2003 to examine coastal circulation during a coral spawning event and to determine if coral larval dispersed from a reef with high coral coverage were reaching some of the nearby reefs with low coral coverage. In this paper, data on the density of coral eggs and planula is compared with in situ acoustic data, oceanographic and meteorologic forcing data, and Lagrangian surface drifter tracks to investigate coral larvae dispersal over a range of timescales. These observations suggest that ADCPs may be useful for long-term, in situ measurement of coral larval spawning and its initial dispersal pathways. Furthermore, the ability to deploy these instruments for long periods of time allows one to put the temporally limited measurements made during a coral spawning event in the context of the longer-term patterns of coastal circulation observed at a site.

Materials and methods

Study area

The island of Maui is located at 20.8°N, 156.5°W in the North-central Pacific between the islands of Molokai, Lanai, Kahoolawe and Hawaii (‘the Big Island’) in the Hawaiian Archipelago (Fig. 1a). West Maui is roughly 30 km long in the north–south direction and on average 20 km wide in the east–west direction. The inner shelf ($<$ 40 m depth) off west Maui in the Pailolo and Auau Channels between the islands of Maui, Lanai and Molokai is highly variable and includes boulders, sand fields and a number of fringing and patch coral reefs along a shoreline facing northwest to southwest (Fig. 1b; Gibbs et al. 2005).

As discussed by Gibbs et al. (2005), areas exposed to large waves in the northern part of the study area are characterized by a thin veneer of coral overlying basaltic substrate, whereas more protected areas typically have coral accreting atop relict reef structures. Reefs extend from the shoreline out to 1 km offshore in water depths of 30 m, but most lay in water depths between 3 and 20 m. Coral coverage is discontinuous (0–80%) along the west Maui coastline (Jokiel et al. 2001), despite the availability of hard substrate (Gibbs et al. 2005) for coral recruitment (Fig. 1b).

The well-developed reefs in the study area are primarily constructed of the corals *Montipora capitata* and *Porites compressa*; these species represent between 18 and 43% of total coral coverage in the study area (Jokiel et al. 2004a). Reefs along this section of coastline have recently been included in the “most impaired” list compiled by the U.S. Environmental Protection Agency for the State of Hawaii (Jokiel et al. 2004a). Indeed, over the past decade, long-term monitoring sites along west

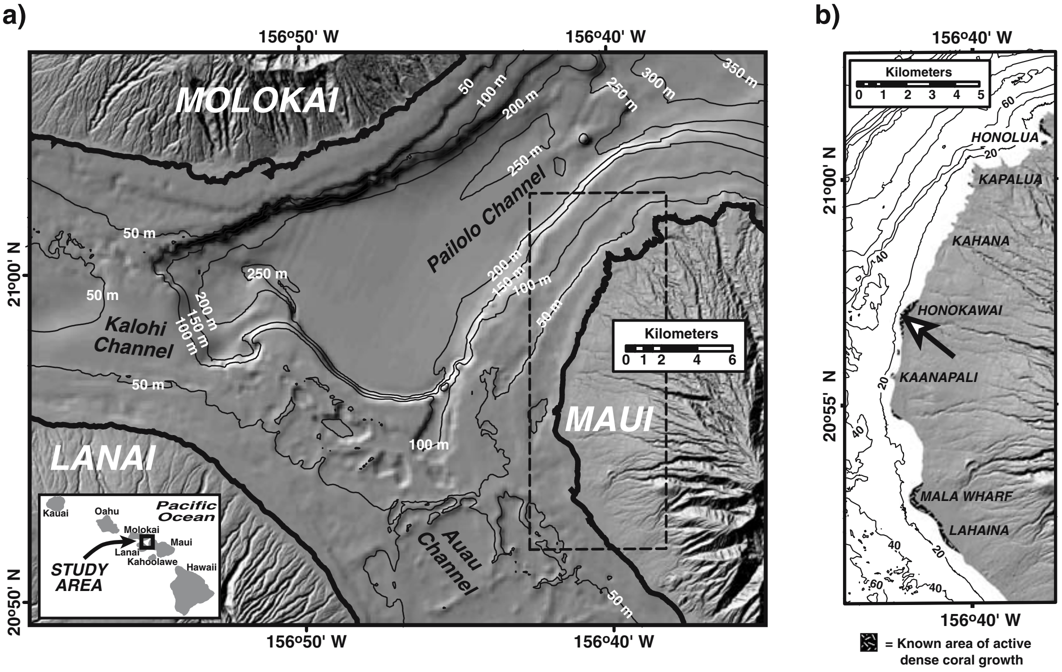

Fig. 1 Maps of the study area. **a** General bathymetry and topography of the study area and its location relative to the eight main Hawaiian Islands. *Dashed box* denotes the area shown in (**b**). **b** USGS high-resolution topography and bathymetry showing the morphology of the study area relative to the approximate areas of known active dense coral growth from our own observations and those by Gibbs et al. (2005). *Arrow* denotes the location of the main study reef at Honokawai. Note the spare nature of active dense coral growth separated by long stretches of suitable coral habitat with no active dense coral growth

Maui have experienced declines in absolute coral cover of 27–35% (Brown 2004; Jokiel et al. 2004b). Consequently, recent attention has focused on processes along the coastline that might explain spatial differences in coral cover and temporal patterns of decline.

This experiment began prior to the onset of *M. capitata* spawning. Heyward (1986) and Kolinski and Cox (2003) identified peak spawning periods for this species around the summer new moon between 20:00 and 22:00 local/Hawaiian Standard Time (HST). In 2003, the first spawning event was predicted to occur from June 29 to July 3. This species was selected because it is one of the major reef builders along this coastline and the egg–sperm bundles are large enough (950–1,050 μm, Mate et al. 1998) to be seen with the naked eye, allowing visual identification of both the initiation and cessation of spawning. Once released from the parent colony, the high lipid content of the eggs (e.g., 60–70% lipid content for congener *Montipora digitata*, Arai et al. 1993) produces positively buoyant egg–sperm bundles that immediately float to the surface (Kolinski 2004). Kolinski (2004) reported that this species usually settles out from the plankton after 3 days but can remain competent for up to 207 days. The large size of the planula larvae (750–1,500 μm, Mate et al. 1998) provides another opportunity to acoustically detect the presence of larvae following the spawning event.

Oceanography and meteorology

There have been a limited number of published studies investigating currents off west Maui. Using satellite altimetry data and a numerical model, Sun (1996) observed weak (0.05–0.10 m s^{-1}) long-term mean eastward flow through the Kalohi and Pailolo Channels, and mean southward flow in the Auau Channel driven by differences in sea surface height across the island chain. Flament and Lumpkin (1996) deployed current meters roughly 25 m below the surface in the Pailolo Channel (water depth ~240 m) for 19 months. They noted that the flow at the shallower current meter was primarily oriented east–west at 0.00–1.00 m s^{-1} (mean = 0.04 m s^{-1}). Storlazzi and Jaffe (2003) made measurements on the inner (< 30 m) shelf and observed that the tides propagate from south to north along west Maui. Their findings, along with those by Flament and Lumpkin (1996), noted that flow was dominated by diurnal and semi-diurnal tidal currents, and to a lesser extent, lower frequency motions driven by the Trade winds.

The Northeast Trade winds occur throughout the year but are most consistent from April–November. These winds strike the northeast side of west Maui, are steered around the west Maui volcanic cone and most often approach the shoreline obliquely from the north in the study area (Fletcher et al. 2002). Insolation-driven heating and nocturnal cooling of the island cause the general Trade wind speeds in the vicinity of the islands to vary from almost negligible at night to more than 10 m s^{-1} in the afternoon, compared to about 5 m s^{-1} in the open ocean. These relatively rapid diurnal variations in wind speed result in a very thin (< 1 m) wind-driven surface layer.

Methods

The hydrographic data used in this study were collected off west Maui in the Kalohi, Pailolo and Auau Channels between the Hawaiian Islands of Maui, Lanai and Molokai (Fig. 1b). A suite of instrument packages was deployed along the 10 m isobath off west Maui to monitor oceanographic and meteorologic variability during the coral spawning season between June 28 and October 2, 2003. Most of the results presented herein are from the instrument package deployed in a sand-filled groove between two coral spurs on the reef at Honokawai. This had four sensors: an upward-looking RD Instruments 614 kHz Workhorse Monitor ADCP, a NIWA Dobie-A wave/tide gauge (DOBIE), an Aqautec/Seapoint 200-TY self-logging optical backscatter (SLOBS) sensor and a Seabird SBE-37SM Microcat conductivity-temperature (CT) sensor (Fig. 2a). The SLOBS and CT sensor sampled every 4 min, while the DOBIE recorded a 512 s burst at 2 Hz at the top of every hour. These sensors collected single-point measurements on optical backscatter, temperature and salinity, and waves and tides, respectively. The ADCP was used to collect vertical profiles of current velocity and acoustic backscatter data every 4 min in 1-m bins from 1 m above the seafloor up past the water surface.

Maximum scattering of acoustic signals is by an object that has a diameter on the order of one-half the wavelength of the acoustic signal (Thorne and Hanes 2002), which, for the 614 kHz ADCP used is this study, corresponds to an optimal scatter size in the range 1,000–1,500 μm (1.0–1.5 mm). As *Monipora capitata* eggs/sperm bundles range from 950–1,050 μm (0.95–1.05 mm) in diameter (Mate et al. 1998), acoustic scattering by the eggs should be detectable with a signal emitted by the 614 kHz ADCP. Other researchers have successfully detected and measured suspended particulate matter concentrations in numerous studies (Holliday and Pieper 1980; Flagg and Smith 1989; Reichel and Nachtnebel 1994; Horne 2000; Jaffe et al. 1999; Holdaway et al. 1999). The raw acoustic backscatter data were corrected for signal strength decay with distance from the transducers due to spreading and absorption using the method outlined by Deines (1999). Following the methodology suggested by Horne (2000) and Holdaway et al. (1999), the corrected acoustic backscatter data is presented as acoustic backscatter, in dB, above the background acoustic backscatter levels. This approach highlights the transient, elevated acoustic backscatter from specific target objects relative to the background noise of the system. Sound speed was assumed to be constant throughout the water column following the observations by Storlazzi et al. (2003) and

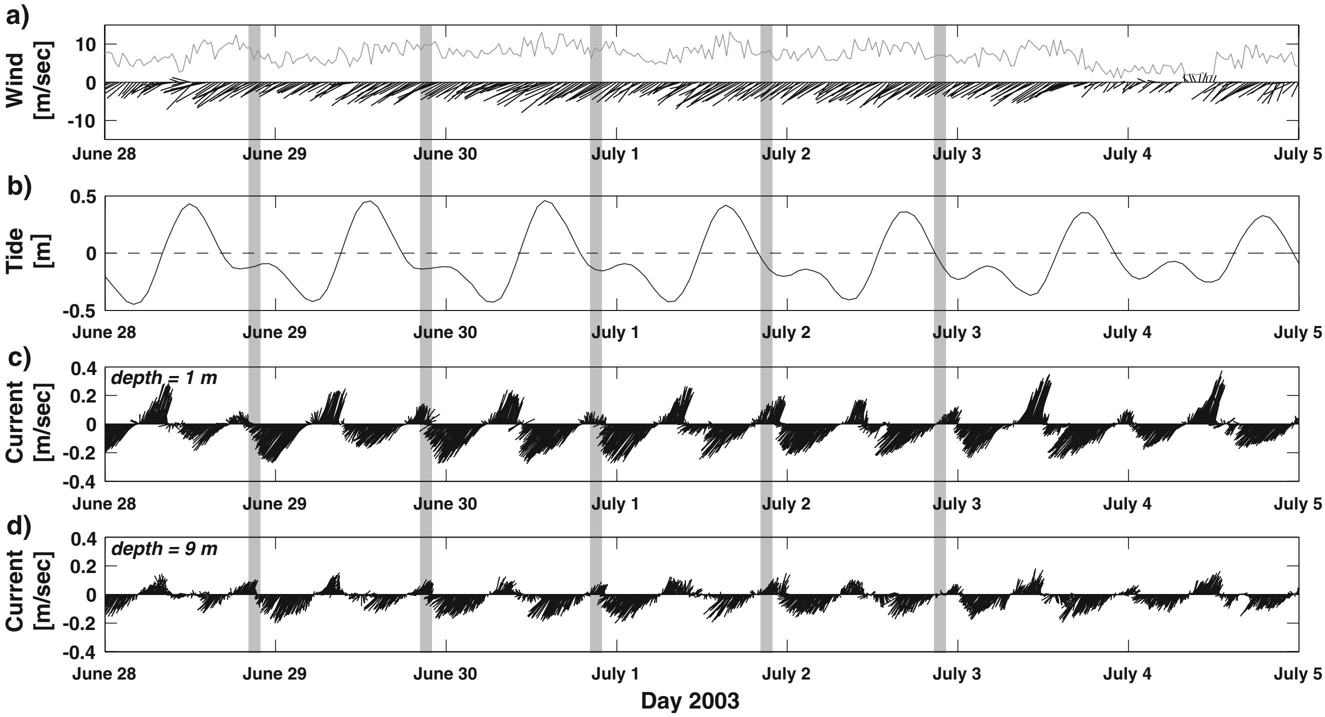

Fig. 2 Meteorologic forcing and the resulting oceanography during the survey period (June 28–July 4). **a** Wind speed and direction. **b** Tidal height. **c** Current speed and direction 1 m below the surface. **d** Current speed and direction 9 m below the surface and 1 m above the seafloor. *Grey bars* denote the times that Kolinski and Cox (2003) predicted *M. capitata* to spawn

was calculated from in situ measurements of temperature, salinity and pressure using the Chen and Millero (1977) method.

Meteorologic data were obtained during the study using a NovaLynx WS-16 weather station mounted approximately 40 m above sea level on top of a hotel roughly 250 m east-southeast of the oceanographic instrument package off Honokawai. Wind speed, wind direction, relative humidity, barometric pressure and precipitation were recorded by the station every half hour. See Storlazzi et al. (2004) for more information on the instrumentation, data acquisition and processing methodology.

Ten differentially equipped Global Positioning System (GPS) radio-tracked drifters were designed and built at the US Geological Survey's Marine Facility in Redwood City, CA (Hatcher et al. 2004). These drifters were deployed during the first major spawning of *M. capitata* during the summer of 2003 between June 28 and July 5. Each drifter was attached directly to a subsurface drogue that extended 0.5 m below the water's surface to make Lagrangian measurements of surface currents. Testing suggested wind-induced slippage of the drifters to be less than 0.02 m s^{-1}; the drifters' positions were recorded every 30 s and the positional accuracies with the differential GPS units were on the order of 3–4 m. These high data rates and spatial accuracies allowed us to understand the Lagrangian pathways at a precision not achieved in previous drifter experiments (Wolanski et al. 1989; Lugo-Fernandez et al. 2001).

Kolinski and Cox (2003) predicted spawning of *M. capitata* to occur between 20:45 and 22:30 HST on the first 4–5 nights following the new moon in May–September. Other *Montipora* species only spawn between the months of July–September, so we therefore choose to focus our efforts on the months of June, July and August, 2003, when we surmised the largest quantities of eggs would be released. For 2003, the predicted *M. capitata* spawning periods during those three months were the nights of June 29–July 2, July 28–August 2, and August 27–31.

On June 28, one day prior to the predicted spawning event, two 4 m^2 plots were established on the reefs immediately adjacent to the instrument package along the 10 m isobath at Honokowai. Thirty *M. capitata* colonies were labeled within each plot using flagging tape and nails. The 4 m^2 plot was considered a maximum size for in situ observation of spawning by one diver and all of the plots had at least 30 colonies. Colonies were defined as discrete structures of living tissue that had discernable physical boundaries.

Beginning on June 29 and continuing until July 2, scuba dives were conducted from 20:30 to 21:45 HST to visually document spawning activity within each of the plots. A dive team consisting of two divers (one per plot), recorded presence/absence of egg/sperm bundles from each of the numbered colonies. No spawning was detected in the plots on July 2, and night dives were discontinued thereafter.

Immediately following the cessation of spawning each night in late June and early July, surface plankton samples were collected at approximately 22:00 HST to estimate relative abundance of the coral egg/sperm bundles and planula larvae. Each night between June 28 and July 3 three replicate plankton tows were made above the site. No tows were made on June 29 due to logistical constraints. Plankton tows were conducted using a 0.50 m diameter, 63 μm mesh net, fitted with a General Oceanics mechanical flowmeter. Tows were parallel to the coastline in a zig–zag pattern that traversed the surface water above and on either side of the seafloor instrument package. Plankton tows ceased two nights after the last in situ spawning was observed. Each 1-l sample collected in the tow was sub-sampled using six raceway trays; the number of eggs and planula were enumerated from each sub-sample, summed and the total was extrapolated for the entire 1-l sample. This method provided nightly averages of eggs and planula density in units of number per volume.

The surface plankton tow data provided an estimate of number of eggs and/or larvae released over the entire time span of the spawning. In order to compare this integrated plankton tow data to the corrected acoustic backscatter data (ABS), we computed the temporal integral of this corrected ABS above the background levels for the time periods (20:45–22:30 HST) when the corals were predicted by Kolinski and Cox (2003) to spawn:

$$\mathrm{ABS}_{\mathrm{spawn}} = \frac{1}{T}\int_{20:45}^{22:30} (\mathrm{ABS}(t) - \min(\mathrm{ABS}))\,\mathrm{d}t$$

with the duration, T, being 105 min. These values of $\mathrm{ABS}_{\mathrm{spawn}}$, in dB, were then compared to the plankton tow data.

Results

The results are presented relative to two time periods: (a) the first major spawning of *M. capitata* between June 28 and July 5, 2003, when the drifters were deployed and larval tows collected; henceforth referred to as the “Survey Period”; and (b) the entire summer spawning season between June 28 and October 2, 2003; henceforth referred to as the “Summer Spawning Season”.

Survey period: June 28–July 5, 2003

Coral spawning

In situ spawning of *M. capitata* colonies in the plots was observed on three nights from June 29 to July 1. No spawning was observed on July 2. Commencement of spawning varied each night from 20:53 HST on June 30 to 21:00 HST on July 1 and lasted until approximately 21:30. Peak spawning in the 10 m plots occurred on June 30 with 25 ± 2% (mean ± SD) of the colonies spawning. Over the three nights, 30% of the colonies in the plots along the 10 m isobath released egg/sperm bundles. The positively buoyant egg/sperm bundles floated slowly (< 0.1 m s^{-1}) upward to the surface and within a few minutes after the cessation of spawning, all of them were constrained to the upper 0.5 m of the water column.

Environmental conditions

Daily insolation-induced Trade wind intensification is evident in the wind speed and wind direction records (Fig. 2a). While the wind speeds were 7.17 ± 2.45 m s^{-1} (mean ± SD), the daily afternoon wind speeds averaged 10–12 m s^{-1}. The survey period encompassed the transition from spring tides at the beginning of the surveys to neap tides by the end (Fig. 2b). The tides off west Maui are of the mixed, semi-diurnal type, with a mean daily tidal range of 0.6 m and minimum and maximum daily tidal ranges of 0.4 and 1.0 m, respectively. See Storlazzi et al. (2004) for more information on the environmental conditions during the 2003 summer coral spawning season.

Current patterns

Most of the daily variability in current speed and direction at the study site during the survey period was due to the tides. During flood tides, currents off west Maui flow to the northeast roughly parallel to shore; conversely, as the tide ebbs, the currents flow to the southwest roughly parallel to shore (Fig. 2c, d). Tidal current speeds close to the surface at the Honokawai site were 0.13 ± 0.08 m s^{-1} (mean ± SD) and 0.07 ± 0.05 m s^{-1} close to the seafloor. The magnitude of the tidal currents is driven by the lunar tidal cycle, with the highest tidal current speeds occurring during the spring tides at the beginning of the survey and the weakest during the neap tides at the end. Superimposed on these northeast–southwest tidally driven current oscillations is a net flow to the southwest under the persistent northeast Trade winds; these current patterns were very consistent during the predicted spawning periods (Fig. 2, grey bars). During the last day and a half of the survey period (July 3–4), however, the winds slackened and there was net flow over the course of the day to the northeast. This pattern occurred after the last of the predicted spawning (Kolinski and Cox 2003) and in situ observed spawning.

Acoustic backscatter

Acoustic backscatter, a measure of scattering material in the water column, was generally more intense and more

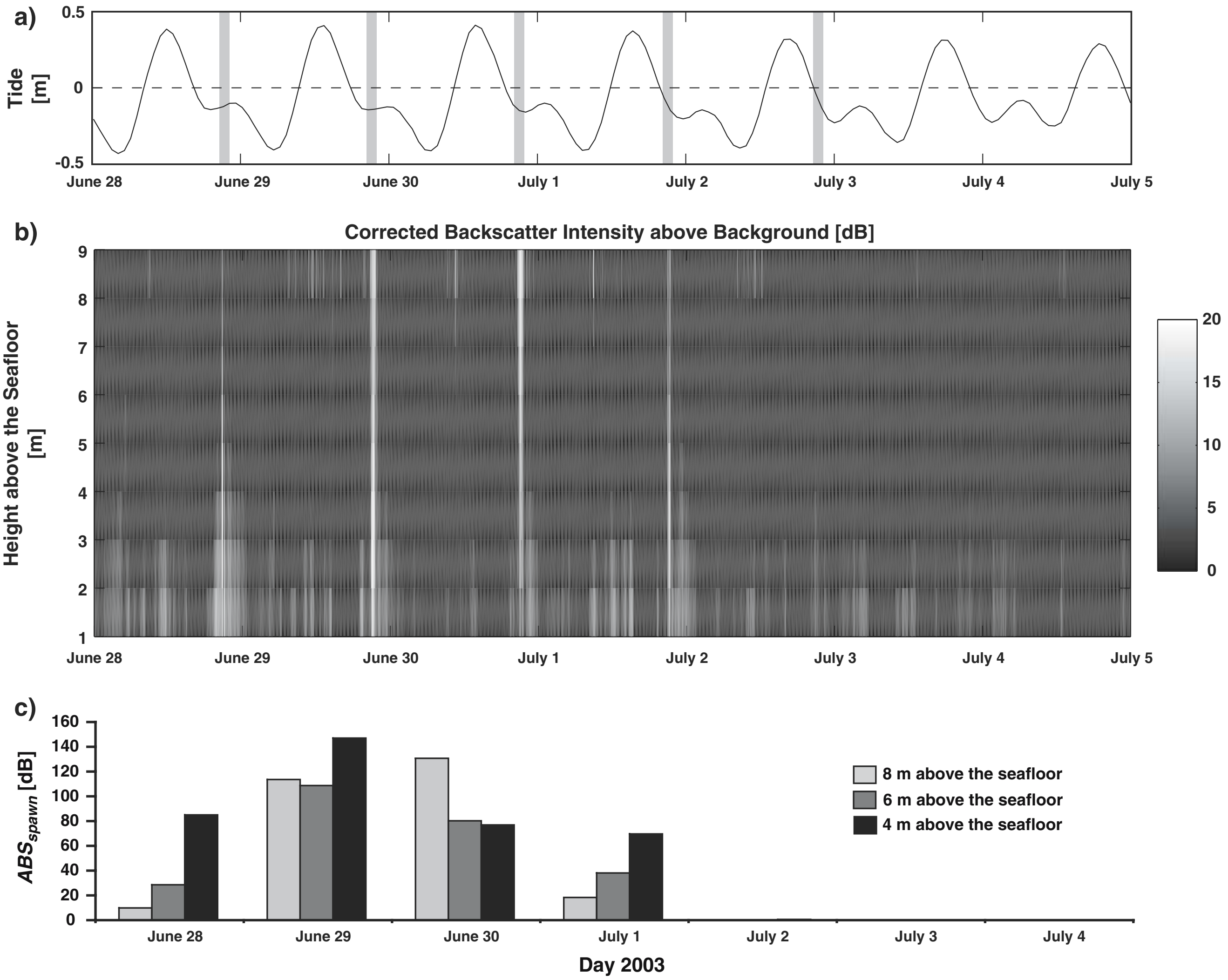

Fig. 3 Acoustic backscatter data during the survey period. **a** Tidal height. **b** Corrected acoustic backscatter above background levels from 1 m above the seafloor up to the surface. **c** $\mathrm{ABS}_{\mathrm{spawn}}$ values for specific water depths. *Grey bars* denote the times that Kolinski and Cox (2003) predicted *M. capitata* to spawn. Note the distinct increases in corrected acoustic backscatter at 21:00–22:00 local/HST on the nights of June 28–July 3 and the correlation of these periods to times of predicted *M. capitata* spawning

variable closer to the bed than higher in the water column during the survey period (Fig. 3). During the lowest points of the tides just before noon each day (Fig. 3a), higher acoustic backscatter was observed close to the bed; the backscatter decreased rapidly upward (Fig. 3b). These periods of elevated near-bed acoustic backscatter were likely due to fine-grained seafloor sediment being resuspended by surface waves driven by the Trade Winds. The water depth was at a minimum during these periods and the ratio of wave height to water depth was at a maximum. At these same times, slightly higher-than-background acoustic backscatter was observed in the upper water column decreasing downward, likely due to air bubbles injected into the surface waters by the breaking of Trade Wind waves. In addition to the trends caused by surface waves, we also observed high acoustic backscatter during the spawning periods. From 21:00 to 22:00 HST on the nights of June 28–July 3, acoustic backscatter was 20–30 dB greater than the background acoustic backscatter from surface waves. Another aspect of these signals during the 21:00–22:00 local (HST) time periods that distinguished them from wave-induced acoustic responses is the relative uniformity of the acoustic backscatter throughout the water column, rather than a rapid decline away from the seafloor (resuspended seafloor sediment) or from the surface (bubbles). For reference, we observed release of *M. capitata* egg/sperm bundles in quantities large enough to cause high optical backscattering of our camera, video and dive lights from 21:00 to 21:30 HST on the nights of June 29–July 1. A surface slick was also visible from vessels during the same time period.

The calculated $\mathrm{ABS}_{\mathrm{spawn}}$ values from the instrument site at 10 m off Honokawai were generally greatest near the bed except during the night of June 30, when $\mathrm{ABS}_{\mathrm{spawn}}$ was greater higher up in the water column

(Fig. 3c). Temporally, ABS$_{spawn}$ increased from June 28 and peaked over the nights of June 29–30, after which it declined to zero on the subsequent nights of July 2–4. Over the nights of June 29–30, ABS$_{spawn}$ was 300–1,000% greater than observed during the previous or subsequent nights of the survey period.

Plankton tows

Plankton tow data were broken down into two categories: eggs and developing planula larvae (Fig. 4). No eggs or planula larvae were recovered by the tows on the night of June 28. The night of June 30 showed the highest number of eggs off the Honokawai site; however, no planula larvae were recovered. From July 1 on through the end of the survey period, decreasing numbers of eggs were recovered until July 4, when no more eggs were recovered in the tows. Planula larvae were first recovered on the night of July 1; their numbers peaked on the night of July 2 and decreased on the night of July 3. No planula larvae were recovered on the night of July 4. The values of ABS$_{spawn}$ higher up in the water column compared very well with the plankton tow data (Fig. 5). The correlations between ABS$_{spawn}$ at both 6 and 8 m above the bed and the egg densities from the plankton tows exceed the 2% level for the sample size (n = 6). Closer to the bed, the correlation between ABS$_{spawn}$ at 4 m above the bed and the egg densities from the plankton tows is not statistically significant, likely due to the addition of backscatter from resuspended seafloor sediment close to the seabed.

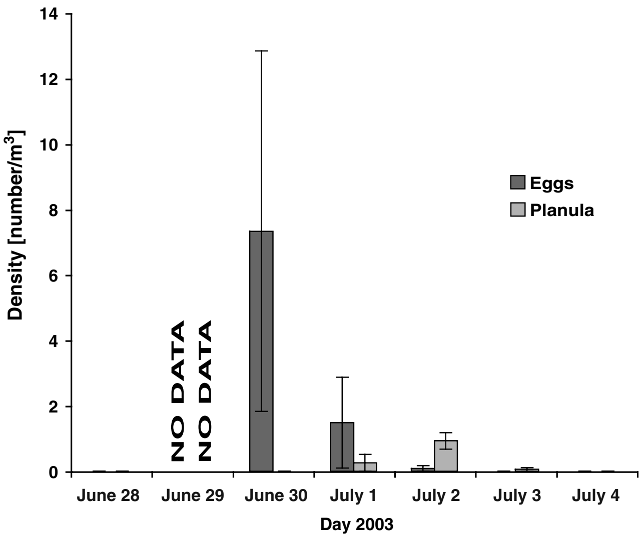

Fig. 4 Variations in the density of coral eggs and planula larvae collected in the plankton tows during the survey period. No data was recovered because of logistical constraints on the night of June 29. Note the similarity between the coral egg densities and the ABS$_{spawn}$ values displayed in Fig. 3c

Projected water and coral larvae pathways

A series of 48-h progressive vector diagrams of projected cumulative flow starting from the study site at 22:00 local time (HST) were constructed using the method described by Siegel et al. (2003) for the nights of June 30–July 2 (Fig. 6). The 48-h duration for these projections was chosen because the majority of the planulae would be carried by the currents for at least 36–48 h before settlement occurred (Babcock and Heyward 1986; Kolinski 2004). These calculations make the assumption that the flow measured at Honokawai is uniform alongshore and across-shore from the instrument site, which is rarely the case (Storlazzi et al. 2003). The projections do, however, provide information regarding the relative direction and magnitude of flow during the projected time period if the forcing mechanisms (wind and tides) were to remain uniform over the projected travel path. Our measurements at the Honokawai site showed that there was net alongshore flow, and therefore net transport of surface water, to the south and offshore to the west. This direction is roughly downwind and parallel to the large-scale bathymetry of the Auau Channel. Observations by Storlazzi et al. (2003) indicate that both wind and current speeds are often 2–3 times greater at distances of 1–2 km offshore, suggesting that these projections underestimate the distance traveled during any given phase of the tide, and that the magnitude of the underestimation likely is greater further

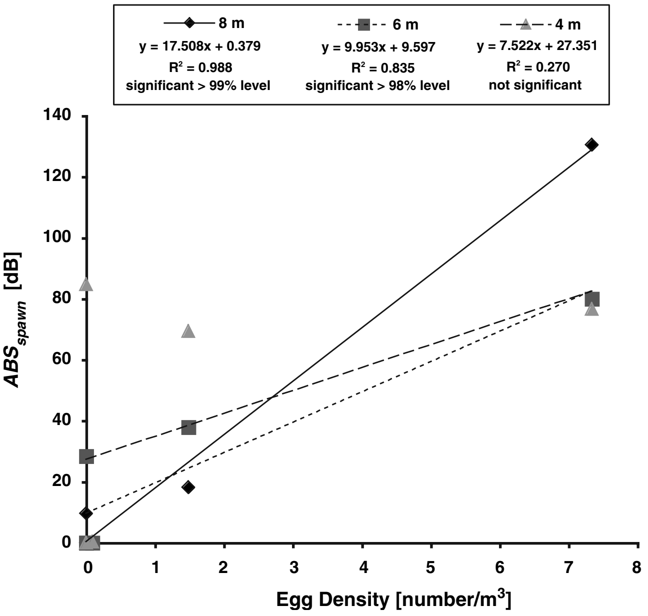

Fig. 5 Relationship between the surface plankton tow data and the ABS$_{spawn}$ values for specific water depths. The correlations between ABS$_{spawn}$ at both 6 and 8 m above the bed and the egg densities from the plankton tows exceed the 2% level; the correlation between ABS$_{spawn}$ at 4 m above the bed and the egg densities from the plankton tows, however, is not statistically significant, as these data are likely contaminated by backscatter from resuspended seafloor sediment

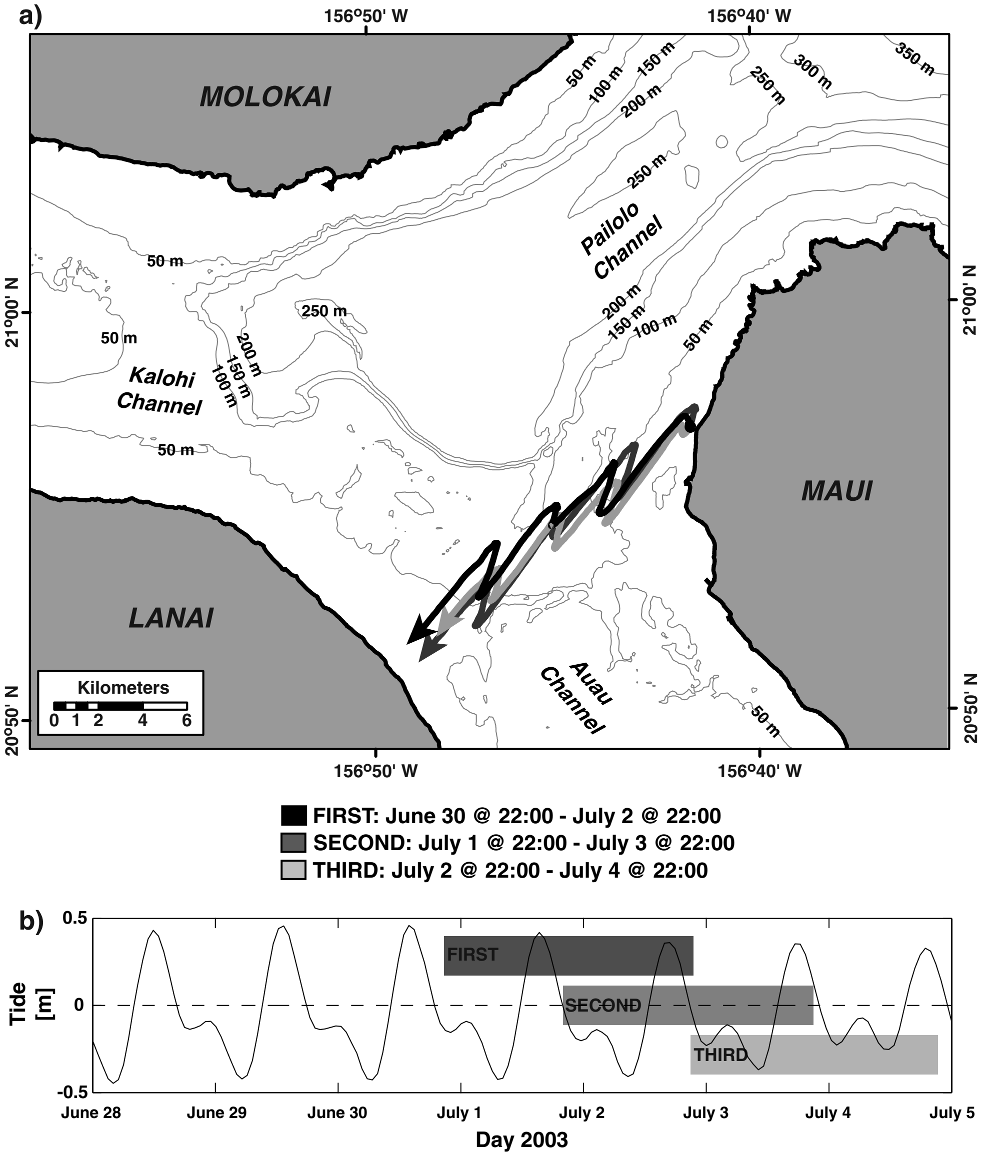

Fig. 6 Projected water and coral larval trajectories over 48 h following coral spawning and the corresponding tidal stages during the survey period. **a** Projected near-surface water mass trajectories over a 48-h period starting at 22:00 local/HST on the specified dates. **b** Tidal stages for the different projections. *Grey bars* denote the periods for each projection. There was net alongshore flow to the south and offshore to the west off the Honokawai site. Observations by Storlazzi et al. (2003) demonstrate that current speeds are greater further offshore, suggesting that coral larvae released from the reefs at this location were transported farther away from the site to the south and west than shown by these projections

offshore. Nevertheless, the projections show that the water masses containing the coral larvae released off Honokawai would have been transported offshore to the southwest, away from the natal reef.

Drifter tracks

The radio-tracked drifters were released from the 10 m reef site and along the 3 m isobath directly inshore of the 10 m site at the cessation of spawning and tracked continuously for the next 12–36 h (Fig. 7). Drifter #1 was released along the 3 m isobath approximately 100 m inshore of the 10 m site; drifters #2, #3 and #5 from the 10 m site; and drifter #4 was released along the 10 m isobath off Kaanapali, roughly 4 km south of the Honokawai site. These drifter releases were designed to determine if the current patterns, which Storlazzi et al. (2003) showed to vary substantially both in the cross-shore and alongshore, would result in drastically different drifter trajectories. See Table 1 for details of the drifter trajectories and speeds.

In general, all of the drifters initially stayed relatively close (within one kilometer or so) to their release points as the tides fluctuated between higher low tide and lower high tide during the first few hours after deployment; mean drifter speeds during this period were on the order of 0.2 m s^{-1}. As the tide fell to the lower low tide, the drifters rapidly moved away from west Maui's coastline. The drifters moved to the southwest at speeds of 0.4–0.8 m s^{-1}during the falling tide, roughly parallel to the 50 m isobath off west Maui, slowed to 0.2–0.3 m s^{-1} as the tides changed, then, in response to the tide rising, reversed and moved rapidly to the northwest at speeds of 0.4–0.8 m s^{-1} roughly parallel to the 50 and 100 m isobaths off northeast Lanai.

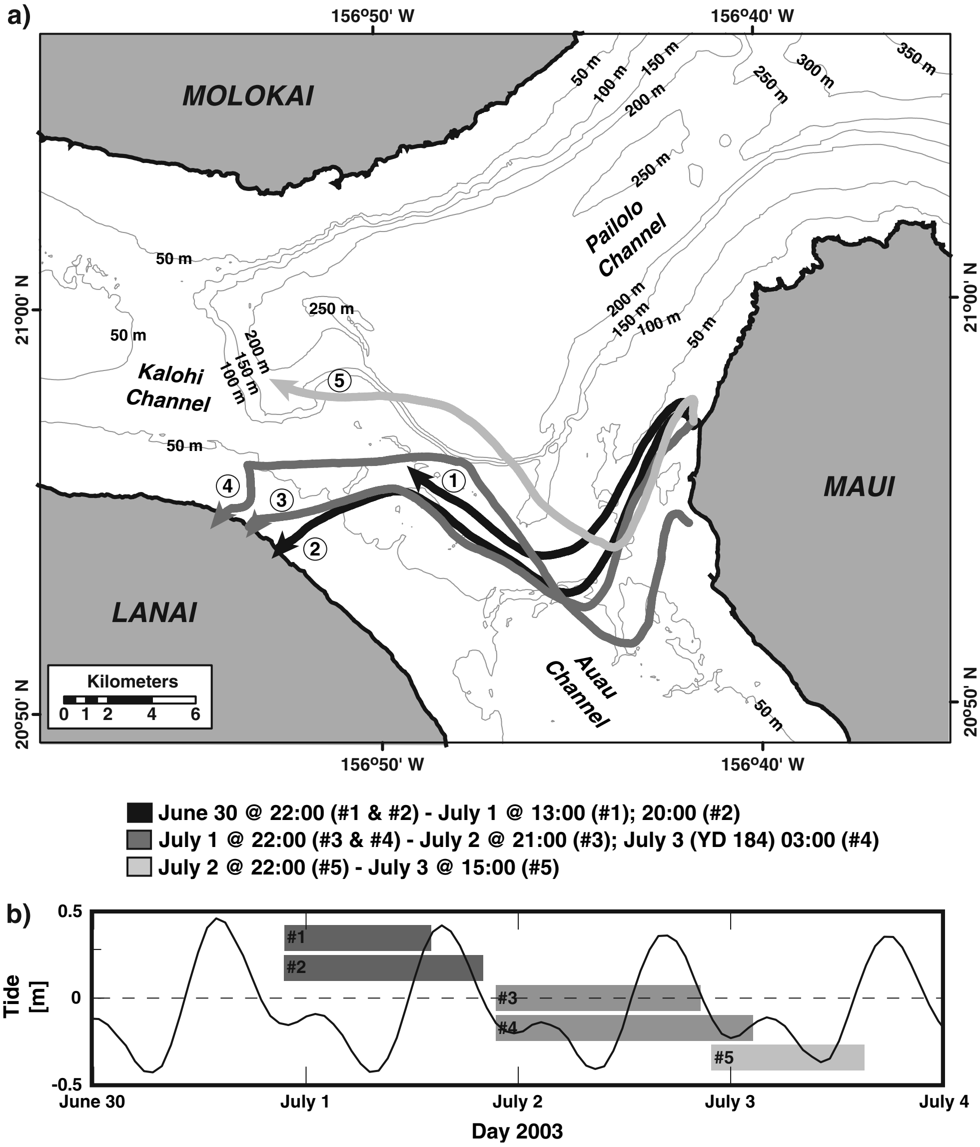

Fig. 7 Drifter tracks and the corresponding tidal stages during the survey period. **a** Map of drifters' tracks in the study area and the approximate dates and times of their deployment and recovery. **b** Tidal stages for the different drifter deployments. *Grey bars* denote the periods of drifter data acquisition. Note the similarity in the drifters' tracks across different days and the projected water and coral larvae trajectories shown in Fig. 6

The northwesterly movement of the surface drifters was oblique to 10–20 m s^{-1} northwest Trade winds; these wind speeds were higher than those shown in Fig. 2, as the wind speeds out in the channels between the islands are often 50–100% faster than those observed along west Maui due to funneling between the islands' large volcanic cones. At higher high tide, the drifters slowed and moved downwind to the west and southwest as the current slacked. Drifter #2 and Drifters #3 and #4, deployed on the nights of June 30 and July 1, respectively, floated onto the large fringing reef off northeast Lanai described by Gulko et al. (2000) and Jokiel et al. (2001). All three of these drifters made the greater than 16 km inter-island transit in less than 28 h, with a mean transit time of 24.29 ± 3.66 h (mean ± SD). Drifter #1 deployed on June 30 was recovered out in the channel by a chase vessel. Drifter #5 traveled on a westward course as the Trade winds weakened (Fig. 2a, c, d), as compared to the southwesterly course the other drifters had taken in the Kalohi Channel under more persistent Trade winds. Note the similarity of these drifters' tracks to the relative magnitude and direction of the ADCP-derived projected current paths shown in Fig. 6.

Summer spawning season: June 28–October 2, 2003

Environmental conditions

Daily insolation-induced Trade wind intensification is evident in the wind speed and wind direction records (Fig. 8a) during the summer spawning season. While the wind speeds were 5.87 ± 3.29 m s^{-1} (mean ± SD), the daily afternoon wind speeds averaged 10–12 m s^{-1}. The summer spawning season encompassed more than seven complete spring-neap tidal cycles (Fig. 8b).

Table 1 Drifter deployment information for the 2003 summer spawning season

Drifter ID	Start				End				Distance traveled (km)	Transit duration (h)	Speed	
	Latitude (deg)	Longitude (deg)	Date	Time (HST)	Latitude (deg)	Longitude (deg)	Date	Time (HST)			Mean (m s^{-1})	Maximum (m s^{-1})
1	20.9505	−156.6937	06/30	22:14	20.9280	−156.8146	07/01	13:02	12.6	14.82	0.37 ± 0.18	1.13
2	20.9501	−156.6929	06/30	22:13	20.9004	−156.8790	07/01	19:43	19.8	21.49	0.41 ± 0.22	2.72
3	20.9507	−156.6936	07/01	22:06	20.9096	−156.8907	07/02	21:04	20.7	22.96	0.39 ± 0.21	1.95
4	20.9088	−156.6964	07/01	23:01	20.9152	−156.9021	07/03	02:44	21.1	28.43	0.37 ± 0.21	1.44
5	20.9507	−156.6936	07/02	22:11	20.9671	−156.8732	07/03	15:05	18.5	16.90	0.35 ± 0.18	1.23

Current patterns

Most of the daily variability in current speed and direction during the summer spawning season was due to the tides (Fig. 8c, d). Tidal current speeds close to the surface at the Honokawai site were 0.18 ± 0.47 m s^{-1} (mean ± SD) and 0.11 ± 0.07 m s^{-1} near the seafloor. The magnitude of the tidal currents is driven by the lunar tidal cycle, with the highest tidal current speeds occurring during the spring tides and the weakest during the neap tides. Deviations in the general trend of northeast–southwest tidal currents with a superimposed net flow to the southwest occurred twice between July 24–28 and September 20–25. During these periods, there was a net flow to the northeast; these occurred concurrently with decreases in wind speed and/or winds out of the south. Similar patterns of net flow to the northeast due to changes in wind forcing were observed off Kahana, roughly 4 km to the north of Honokawai during 2002 (Storlazzi and Jaffe 2003). During the in situ observations of spawning (June 28–July 2) and both of the later spawning events (July 29–August 2 and August 27–31) predicted by Kolinski and Cox (2003), currents measured at the Honokawai site were generally northeast–southwest tidal currents with net flow to the southwest. This flow pattern is consistent with observations made throughout 2002 (Storlazzi and Jaffe 2003).

Projected water and coral larvae pathways

A series of 48-h progressive vector diagrams of projected cumulative flow, using the methodology described by Siegel et al. (2003), for all of the predicted periods of *M. capitata* spawning during the summer of 2003 were computed (Fig. 9). These data project near-surface water mass trajectories over a 48-h period starting at 22:00 local time (HST) on June 28–July 2 (Fig. 9a), July 29–August 2 (Fig. 9b), and August 27–31 (Fig. 9c). These dates correspond to the periods when coral spawning was observed or predicted by Kolinski and Cox (2003). These data show that there was net alongshore flow to the south and offshore to the west off the Honokawai site, causing net projected transport of surface water to be to the south and offshore. Observations by Storlazzi et al. (2003) demonstrate that current speeds are greater offshore than close to the reef, indicating that these projections are minimal values for water mass and likely larval transport. These projections again are similar to the drifter data collected during the June 28–July 2 spawning (Fig. 7).

Discussion

In the main eight Hawaiian Islands connectivity within the marine ecosystem has been documented for specific species (Ziegler 2002), but the spatial and temporal patterns have not previously been clarified. The results

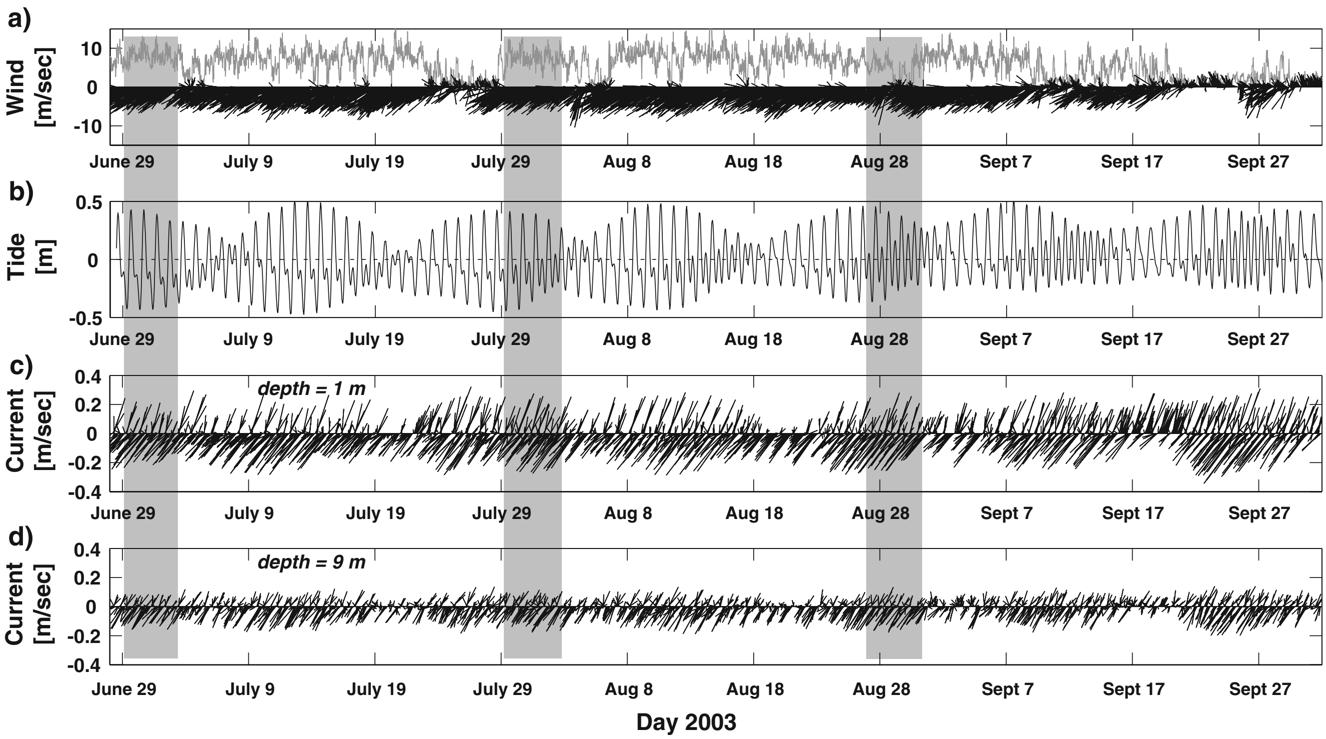

Fig. 8 Meteorologic forcing and the resulting oceanography during the summer spawning season (June 28–October 2). **a** Wind speed and direction. **b** Tidal height. **c** Current speed and direction 1 m below the surface. **d** Current speed and direction 9 m below the surface and 1 m above the seafloor. *Grey bars* denote the times that Kolinski and Cox (2003) predicted *Montipora capitata* to spawn. Note the similarity of the meteorologic and oceanographic data during the three coral spawning periods

of this study documented in situ spawning of an abundant coral species in Hawaii and used various techniques to infer initial dispersal of coral larvae from a reef system. Investigating environmental conditions also revealed consistent patterns of water flow and direction suggesting that the observations in this study may be representative of annual spawning periods.

The meteorologic and oceanographic data from both this study and previous studies (Flament and Lumpkin 1996; Storlazzi and Jaffe 2003) show that flow off west Maui in the Auau, Pailolo and Kalohi Channels is primarily controlled by the winds and tides. The general flow patterns and seawater properties show greater consistency during the summer months when the forcing by Northeast Trade winds is relatively steady, storms occur very infrequently and nearshore surface wave-induced flows are at a minimum. During both the survey period (June 28–July 5) and the summer coral spawning season (June 28–October 2), both the forcing (winds and tides) and the resulting flow and environmental patterns were relatively consistent, with northeast–southwest oscillating tidal currents with a superimposed net flow to the southwest and offshore. Similar forcing and response across multiple spawning periods resulted in comparable models of projected water and coral larvae pathways during the 2003 spawning season. Furthermore, since *M. capitata* always spawns the nights following a new moon, these spawning events always occur during the transition from spring to neap tides and thus the relative magnitude of the tidal current forcing during each spawning period is relatively consistent. These consistent patterns, along with the similar paths that the drifters followed over multiple deployments, suggest that the temporally limited drifter trajectories from the survey period (June 28–July 5) are likely a good model for initial dispersal patterns off west Maui during the summer months when many of the Hawaiian corals spawn.

As the density of coral eggs or developing planula larvae was not measured along the drifter tracks after the drifters were released, the results of larvae transport are preliminary. Wolanski et al. (1989) and Willis and Oliver (1988) suggest, however, that drifters can accurately mimic larval dispersal at timescales of up to 5 days. The temporally limited but spatially extensive measurements made during the survey period, in conjunction with the long-term, spatially limited measurements made over the summer spawning season and previous studies, suggest that this reef off is likely not self-seeding over relatively short (0 h to days) timescales. While larval competency and dispersal potential for many coral species can be quite high (Richmond 1987, 1988; Wilson and Harrison 1998; Kolinski 2004), Miller and Mundy (2003) suggest that dispersal of broadcast-spawning corals may be not as great as previously assumed. If this is the case, the short timescales of dispersal shown here are important because both larval density and recruitment success decrease quickly with time and distance (Sammarco and Andrews 1988) due to

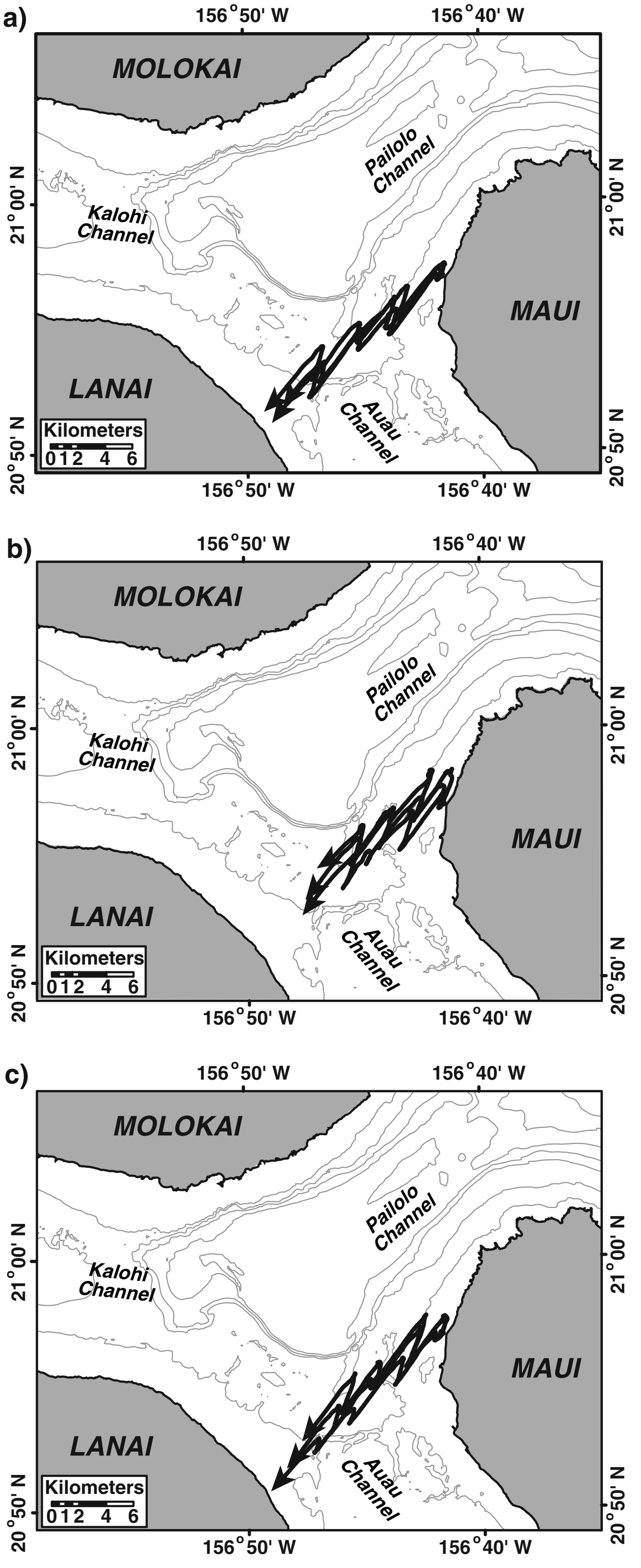

◀

Fig. 9 Projected water mass and coral larval trajectories over 48 h following the periods of coral spawning predicted by Kolinski and Cox (2003) for the summer spawning season. **a** June 28–July 2. **b** July 29–August 2. **c** August 27–31. These data show projected near-surface water mass trajectories over a 48-h period starting at 22:00 local/HST on the specified dates. There was net flow to the southwest off the Honokawai site for all of the predicted *M. capitata* spawning periods in 2003. This and other data suggest that coral larvae released from the reefs at this location were transported farther away from the site to the south and west than shown by these projections

mixing and horizontal dispersion (e.g., Wolanski et al. 1989; Oliver et al. 1992).

While the application of acoustic backscatter for measurements of particulate matter in the water column is not new, these results suggest that ADCPs can also be used to make qualitative measurements of coral spawning. By conducting co-located plankton tows during a spawning period and comparing the egg density results with the near-surface acoustic response of an ADCP, it may also be possible to make quantitative measurements of coral spawning. ADCPs, which are becoming the standard for current measurements in the coastal zone, thus permit researchers to not only make long-term, in situ measurements of current speed and direction, but if the acoustic backscatter is properly corrected for beam spreading and attenuation, one could also make long-term, remotely sensed measurements of coral spawning. The benefits from such an approach are twofold. First, it would allow scientists to easily document the relative intensity and duration of multiple episodes of coral spawning without numerous trips into the field. Second, the concurrent current information provides insight into the initial dispersal direction of coral larvae and developing planula. These trajectories can then be viewed in the context of the flow patterns observed over the length of the instrument's deployment, allowing scientists to know if their limited field observations are representative of the system.

Acknowledgements This work was carried out as part of the USGS's Pacific Coral Reef Project, an effort in the U.S. and its trust territories to better understand the effect of geologic processes on coral reef systems. Andrea Ogston (UW), Kathy Presto, Dave Gonzales, Tom Reiss, Gerry Hatcher, Josh Logan (USGS), Allan Ligon (UH), Donna Brown (MCCC), Skippy Hau (HI-DAR) and Joe Reich, the captain of the *R/V Alyce C.*, deserve special credit for committing an enormous amount of time and effort into all aspects of the fieldwork. We would also like to thank Jessica Lacy, Amy Draut (USGS), Richard Dunne the reviewers at Coral Reefs who contributed numerous excellent suggestions and a timely review of our work. Use of trademark names does not imply USGS endorsement of products.

References

Arai T, Kato M, Heyward A, Ikeda Y, Iizuka T, Maruyama T (1993) Lipid composition of positively buoyant eggs of reef building corals. Coral Reefs 12:71–75

Babcock RC, Heyward AJ (1986) Larval development of certain gamete-spawning scleractinian corals. Coral Reefs 5:111–116

Brown EK (2004) Reef coral populations: spatial and temporal differences observed at six reefs off West Maui. Ph.D. thesis, Zoology, University of Hawaii, Honolulu, p 277

Chen CT, Millero FJ (1977) Speed of sound in seawater at high pressures. J Acoust Soc Am 62:1129–1135

Deines KL (1999) Backscatter estimation using broadband acoustic Doppler current profilers. In: Proceedings 6th IEEE working conference on current measurement, pp 249–253

Fabricius KE (2005) Effects of terrestrial runoff on the ecology of corals and coral reefs: review and synthesis. Mar Pollut Bull 50:125–146

Flagg CN, Smith SL (1989) On the use of the acoustic Doppler current profiler to measure zooplankton abundance. Deep-Sea Res 36:455–474

Flament P, Lumpkin C (1996) Observations of currents through the Pailolo Channel: implications for nutrient transport. In: Wiltse W (ed) Algal blooms: progress report on scientific research. West Maui Watershed Management Project, State of Hawaii Department of Health, Honolulu, pp 57–64

Fletcher CH, Richmond BM, Grossman EE, Gibbs AE (2002) Atlas of natural hazards in the Hawaiian Coastal Zone. USGS Geologic Investigations Series I-2716

Gibbs AE, Grossman EE, Richmond BM (2005) Summary and preliminary interpretations of USGS cruise A202HW: underwater video surveys collected off Oahu, Molokai and Maui, Hawaii, June–July, 2002. U.S. Geological Survey Open-File Report 2005-1244 http://www.pubs.usgs.gov/of/2005/1244/

Grigg RW, Maragos JE (1974) Recolonization of hermatypic corals on submerged lava flows in Hawaii. Ecology 55:387–395

Gulko D, Maragos J, Friedlander AM, Hunter C, Brainard R (2000) Status of coral reefs in the Hawaiian Archipelago. In: Wilkinson C (ed) Status of coral reefs of the world: 2000, Australian Institute of Marine Science, Townsville, pp 219–238

Hatcher GA, Reiss TE, Storlazzi CD (2004) Application of GPS drifters to track Hawaiian coral spawning. U.S. Geological Survey Open-File Report 2004–1309 http://www.pubs.usgs.gov/of/2004/1309/

Heyward AJ (1986) Sexual reproduction in five species of the coral *Montipora*. In: Jokiel PL, Richmond RH, Rogers RA (eds) Coral reef population biology. Hawaii Institute of Marine Biology, Kaneohe, Oahu. Technical Report 37, pp 170–178

Holdaway GP, Thorne PD, Flatt D, Jones SE, Prindle D (1999) Comparison between ADCP and transmissometer measurements of suspended sediment concentration. Cont Shelf Res 19:421–441

Holliday DV, Pieper RE (1980) Volume scattering strengths and zooplankton distributions at acoustic frequencies between 0.5 and 3 MHz. J Acoust Soc Am 67:135–146

Horne JK (2000) Acoustic approaches to remote species identification: a review. Fish Oceanogr 9:356–371

Jaffe JS, De Robertis A, Ohman MD (1999) Sonar estimate of daytime activity levels of Euphausia pacifica in Saanich Inlet. Can J Fish Aquat Sci 56:2000–2010

Jokiel PL, Brown EK, Friedlander AM, Rodgers SK, Smith WR (2001) Hawaii Coral Reef Initiative Coral Reef Assessment and Monitoring Program (CRAMP) final report 1999–2000, University of Hawaii, Honolulu

Jokiel PL, Rodgers KS, Brown EK (2004a) Assessment, mapping, and monitoring of selected "most impaired" coral reef areas in the State of Hawaii. Environmental Protection Agency, Honolulu

Jokiel PL, Brown EK, Friedlander AM, Rodgers SK, Smith WR (2004b) Hawaii coral reef assessment and monitoring program: spatial patterns and temporal dynamics in reef coral communities. Pac Sci 58:159–174

Kolinski SP (2004) Sexual reproduction and the early life history of *Montipora capitata* in Kaneohe Bay, Oahu, Hawaii. Ph.D. thesis, Zoology, University of Hawaii, Honolulu, Hawaii, p 152

Kolinski SP, Cox EF (2003) An update on modes and timing of gamete and planula release in Hawaiian Scleractinian corals with implications for conservation and management. Pac Sci 57:17–27

Loya Y (1976) Recolonization of Red Sea corals affected by natural catastrophes and man-made perturbations. Ecology 57:278–289

Lugo-Fernandez A, Deslarzes KJP, Price JM, Boland GS, Morin MV (2001) Inferring probable larval dispersal of Flower Garden Banks coral larvae (Gulf of Mexico) using observed and simulated drifter trajectories. Cont Shelf Res 21:47–67

Mate JL, Wilson J, Field S, Neves EG (1998) Fertilization dynamics and larval development of the scleractinian coral *Montipora verrucosa* in Hawai'i. In: Cox EF, Krupp DA, Jokiel PL (eds) Reproduction in reef corals. Hawaii Institute of Marine Biology, Kaneohe, Technical report 42, pp 27–39

Miller K, Mundy C (2003) Rapid settlement in broadcast spawning corals: implications for larval dispersal. Coral Reefs 22:99–106

Nadaoka K, Harii S, Mitsui J, Tamura H, Hanada G, Paringit E, Nihei Y, Fujii S, Sato K, Matsuoka T, Kakuma S, Ikema T, Iwao K, Takahashi T (2002) Larval tracking using small drifters and larval settling experiments to examine long-distance larval transport of corals. Proc Japanese Coastal Engineering Conference, Japanese Society of Civil Engineers 49:366–370

Oliver JK, King BA, Willis BL, Babcock RC, Wolanski E (1992) Dispersal of coral larvae from a lagoonal reef- II: Comparisons between model predictions and observed concentrations. Cont Shelf Res 12:873–889

Reichel G, Nachtnebel HP (1994) Suspended sediment monitoring in a fluvial environment: advantages and limitations of applying an acoustic Doppler current profiler. Water Res 28:751–761

Richmond RH (1987) Energetics, competency, and long-distance dispersal of planula larvae of the coral *Pocillopora damicornis*. Mar Biol 93:527–533

Richmond RH (1988) Competency and dispersal potential of planula larvae of a spawning versus a brooding coral. Proc 6th Int Coral Reef Symp 2:827–831

Sammarco PW, Andrews JC (1988) Localized dispersal and recruitment in Great Barrier Reef corals: the helix experiment. Science 239:1422–1424

Siegel DA, Kinlan BP, Gaines SD (2003) Lagrangian descriptions of marine larval dispersion. Mar Ecol-Prog Ser 260:83–96

Storlazzi CD, Jaffe BE (2003) Coastal circulation and sediment dynamics along West Maui, Hawaii, PART I: Long-term measurements of currents, temperature, salinity and turbidity off Kahana, West Maui: 2001–2003. U.S. Geological Survey Open-File Report 03-482 http://www.pubs.usgs.gov/of/2003/of03-482/

Storlazzi CD, Logan JB, McManus MA, McLaughlin BE (2003) Coastal circulation and sediment dynamics along West Maui, Hawaii, PART II: Hydrographic Survey Cruises A-3-03-HW and A-4-03-HW Report on the spatial structure of currents, temperature, salinity and turbidity along Western Maui. U.S. Geological Survey Open-File Report 03-430 http://www.pubs.usgs.gov/of/2003/of03-430/

Storlazzi CD, Field ME, Ogston AS, Logan JB, Presto MK, Gonzales DG (2004) Coastal circulation and sediment dynamics along West Maui, Hawaii, PART III: Flow and particulate dynamics during the 2003 summer coral spawning season. U.S. Geological Survey Open-File Report 2004-1287 http://www.pubs.usgs.gov/of/2004/1287/

Sun LC (1996) The Maui algal bloom: the role of physics. In: Wiltse W (ed) Algal blooms: progress report on scientific research. West Maui Watershed Management Project, State of Hawaii Department of Health, Honolulu, pp 54–57

Swearer SE, Shima JS, Hellber ME, Thorrold SR, Jones GP, Robertson DR, Morgan SG, Selkoe KA, Ruiz GM, Warner RR (2002) Evidence of self-recruitment in demersal marine populations. B Mar Sci 70:S251–S271

Thorne PD, Hanes DM (2002) A review of acoustic measurements of small-scale sediment processes. Cont Shelf Res 22:603–632

Willis BL, Oliver JK (1988) Inter-reef dispersal of coral larvae following the annual mass spawning on the Great Barrier Reef. Proc 6th Int Coral Reef Symp 2:853–859

Wilson JR, Harrison PL (1998) Settlement-competency periods of larvae of three species of scleractinian corals. Mar Biol 131:339–345

Wolanski E, Burrage D, King B (1989) Trapping and dispersion of coral eggs around Bowden Reef, Great Barrier Reef, following mass coral spawning. Cont Shelf Res 9:479–496

Ziegler AC (2002) Hawaiian natural history, ecology, and evolution. University of Hawaii Press, Honolulu, Hawaii